

Electronic Supplementary Information (ESI)

Simple defect engineering of carbon nitride using mixed precursors for enhanced photocatalysis

1. Reagent

2,4,6-Triamino-1,3,5-triazine (99%, Sigma-Aldrich), 2,4-diamino-6-phenyl-1,3,5-triazine (97%, Sigma-Aldrich), benzyl alcohol (99.5%, ChemPure), benzaldehyde ($\geq 99.5\%$, ChemPure), potassium iodide ($\geq 99.5\%$, ChemPure), potassium chloride ($\geq 99.5\%$, Merck), sodium hydroxide ($\geq 97\%$, Merck), 5,5-dimethyl-1-pyrroline N-oxide, DMPO ($\geq 99\%$, Sigma-Aldrich), 2,2,6,6-tetramethylpiperidine-1-oxyl, TEMPO (99%, Sigma-Aldrich), 2,2,6,6-Tetramethylpiperidine, TEMP ($\geq 99\%$, Sigma-Aldrich), 1,4-benzoquinone ($\geq 98\%$, Sigma-Aldrich), silver nitrate (99.8%, Stanlab), *tert*-butanol ($\geq 99\%$, Carl Roth), Cu₂O (99.5%, FUJIFILM Wako), and CuO (99.9%, FUJIFILM Wako) were used as received. Ultrapure water the Milli-Q® system was used throughout all the experiments.

2. Synthesis

Defective CN (d-CN) was synthesized by co-polymerizing 2,4,6-triamino-1,3,5-triazine (M1) with 4-diamino-6-phenyl-1,3,5-triazine (M2), where M2 functions as an end-capping monomer (Figure S1). The synthesis involved ultrasonically mixing M2 (0.167 g) with M1 (1.5 g) at 40 kHz for 2 h in 50 mL of ultrapure water (Milli-Q). After the solvent had completely evaporated, the mixture was transferred into a silica crucible and then calcined at 550 °C for 4 h under a flux of KCl/NaOH in an Ar flow of 1 L min⁻¹. The amounts of KCl and NaOH were 5 g and 0.1 g, respectively. After cooling to room temperature, the resulting powder was ground using an agate mortar and washed with water until the rinse water reached a neutral pH. The final product was dried under vacuum at 80 °C for 12 h. As a control, CN was prepared using the same protocol, but without the addition of M2.

3. Characterization

The microstructure was analyzed using XRD (Bruker D8). Morphological characteristics were observed using TEM (Talos F200X, FEI). The specific surface area was determined with an adsorption analyzer (Belsorp 28SA, Bel). CO₂ and NH₃ adsorption on the photocatalysts were measured by TPD using a chemisorption analyzer (ChemiSorb 2750, Micromeritics). Optical properties were determined by recording DRS spectra with a UV-Vis-NIR spectrophotometer (Lambda 950, PerkinElmer). TRMC measurements were performed using the third harmonic (450 nm) of a Nd:YAG laser (Vibrant II, Opotek) for photoexcitation. X-ray photoelectron spectroscopy was conducted with a PHI 5000 VersaProbe (ULVAC-PHI).

4. Evaluation

The photocatalytic activity for the selective oxidation of BA to BAL was evaluated in a batch reactor. Details regarding the reactor configuration can be found in our previous reports.^{1, 2} In each experiment, 5 mg of photocatalyst was dispersed in 10 mL of BA (1 mmol L⁻¹), with ultrapure water serving as the solvent. The reaction mixture was continuously stirred using a magnetic stirrer and allowed to stabilize for 1 hour before being exposed to irradiation from a 455 nm LED lamp. The temperature was kept constant at 25 °C by submerging the setup in a water bath. After 3 h of irradiation, a 0.15 mL sample was evacuated, filtered through a nylon membrane, and analyzed using a gas chromatograph (GC-2010 Shimadzu) equipped with a flame ionization detector. To investigate catalyst reusability, the material was recovered after each experiment by removing the solvent, rinsing it three times with water, drying it at 100 °C for 24 h, and then reusing it in a fresh BA solution for the subsequent run. Scavenger experiments were conducted to determine the reactive species responsible for BAL formation by introducing specific scavengers immediately after

turning on the lamp. The photocatalytic performance, including BA conversion, BAL yield, and BAL selectivity, was determined using the following equations.

$$\text{Conversion (\%)} = \left(\frac{C_0 - C_r}{C_0} \right) \times 100 \quad (1)$$

$$\text{Yield (\%)} = \left(\frac{C_p}{C_0} \right) \times 100 \quad (2)$$

$$\text{Selectivity (\%)} = \left(\frac{C_p}{C_0 - C_r} \right) \times 100 \quad (3)$$

$$\text{Aromatic balance (\%)} = \left(\frac{C_r + C_p}{C_0} \right) \times 100 \quad (4)$$

where C_0 is the initial BA concentration (mmol L^{-1}). C_r and C_p are the concentration of reactant (BA) and product (BAL) when sampling, respectively.

5. DFT Calculations

The CN framework, characterized by a C/N stoichiometry of 0.75, was modeled by arranging three heptazine units to create a carbon nitride cluster ($\text{C}_{18}\text{N}_{27}\text{H}_8$) containing a cavity and uncondensed - NH_2 groups, based on previous studies.^{3,4} One -OH group is attached to one of the heptazine units to replace one - NH_2 group. In d-CN, a phenyl group is attached to one of the heptazine units, thereby disconnecting two heptazine units to simulate a defective CN framework. Computational calculations with DFT were conducted using ORCA 6, which utilizes the SHARK integral generation and digestion engine.^{5,6} The Becke, 3-parameter, Lee–Yang–Parr (B3LYP) hybrid functional was employed, while triple-zeta valence (TZV) basis sets were applied with strict convergence criteria. Excited-state calculations were carried out using time-dependent density functional theory (TD-DFT), with analysis performed via Multiwfn software.^{7,8} The results were then visualized using Chemcraft software.⁹

6. Determination of Apparent Quantum Yield

The apparent quantum yield (AQY) was calculated using the following equation.

$$\text{AQY (\%)} = \left(\frac{2\nu N_A h c}{I A \lambda} \right) \times 100 \quad (5)$$

where ν is the rate of BAL production (mol s^{-1}), N_A is the Avogadro's number ($6.02 \times 10^{23} \text{ mol}^{-1}$), h is Planck's constant ($6.62 \times 10^{-34} \text{ J s}$), c is the speed of light ($3.0 \times 10^8 \text{ m s}^{-1}$), I is the light intensity (1513 W m^{-2}), A is the irradiation area ($1.25 \times 10^{-5} \text{ m}^2$), and λ is the light wavelength (455 nm).

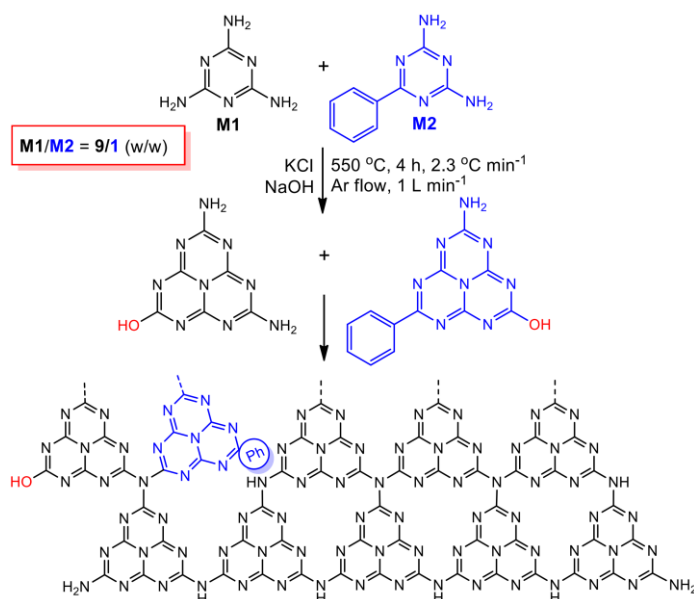


Fig. S1 Schematic illustration of the synthesis route of d-CN. CN is obtained in the absence of the M2 precursor.

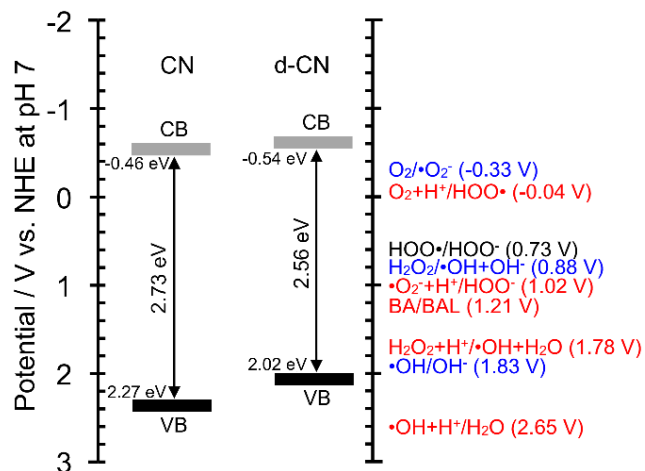


Fig. S2 Electronic band structure determined from UPS and DRS spectra. The standard redox potentials (E^0) are taken from Ref. 10-13. Redox couples written in red, blue, and black indicate that the corresponding redox reactions tend to occur under acidic, basic, and neutral conditions, respectively.

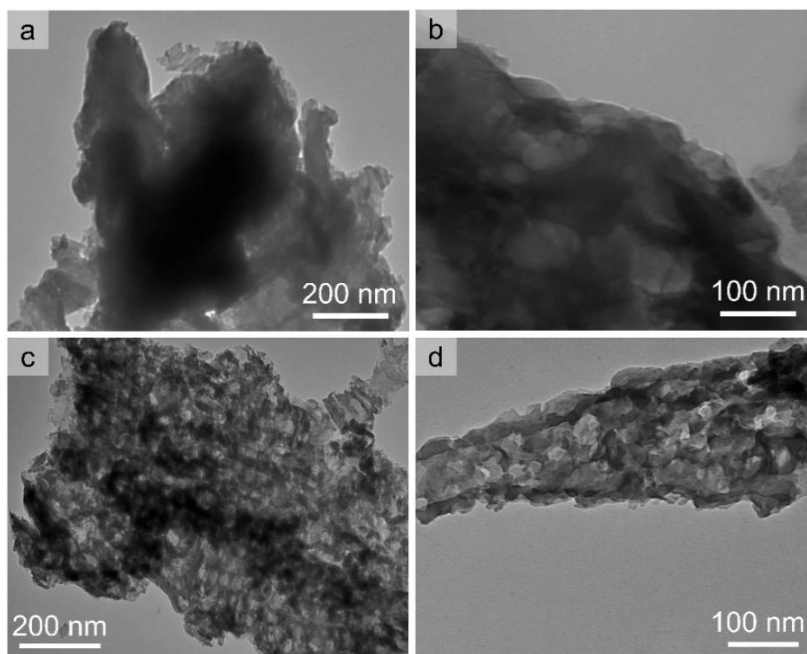


Fig. S3 TEM images of CN (a, b) and d-CN (c, d) from different areas.

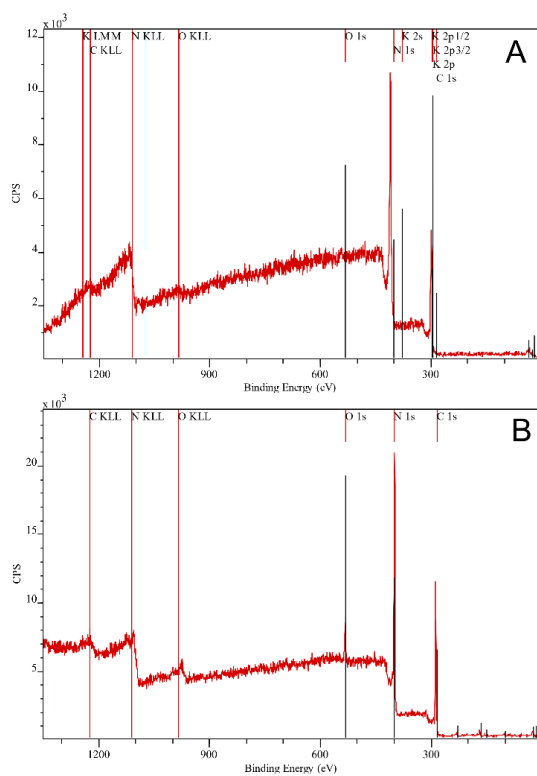


Fig. S4 XPS survey scan of (A) CN and (B) d-CN.

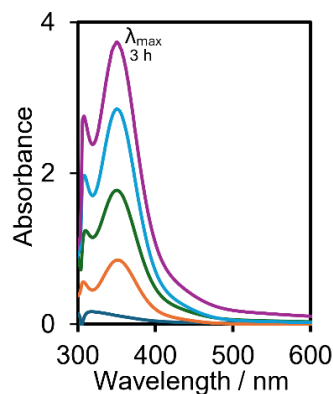


Fig. S5 An example of product determination during the photocatalytic evaluation of d-CN in the presence of BA in water at 455 nm. H_2O_2 and BAL are detected as oxidation products. H_2O_2 is determined iodometrically. The iodometric method for H_2O_2 determination is based on its reaction with iodide (I^-) in an acidic medium, forming triiodide (I_3^-) according to the equation: $\text{H}_2\text{O}_2 + 3\text{I}^- + 2\text{H}^+ \rightarrow \text{I}_3^- + 2\text{H}_2\text{O}$. The generated I_3^- exhibits a characteristic UV-light absorption at a maximum wavelength (λ_{max}) of 351 nm. By measuring the absorbance at this wavelength using a UV-Vis spectrophotometer, the concentration of I_3^- can be correlated with the amount of H_2O_2 in the sample.

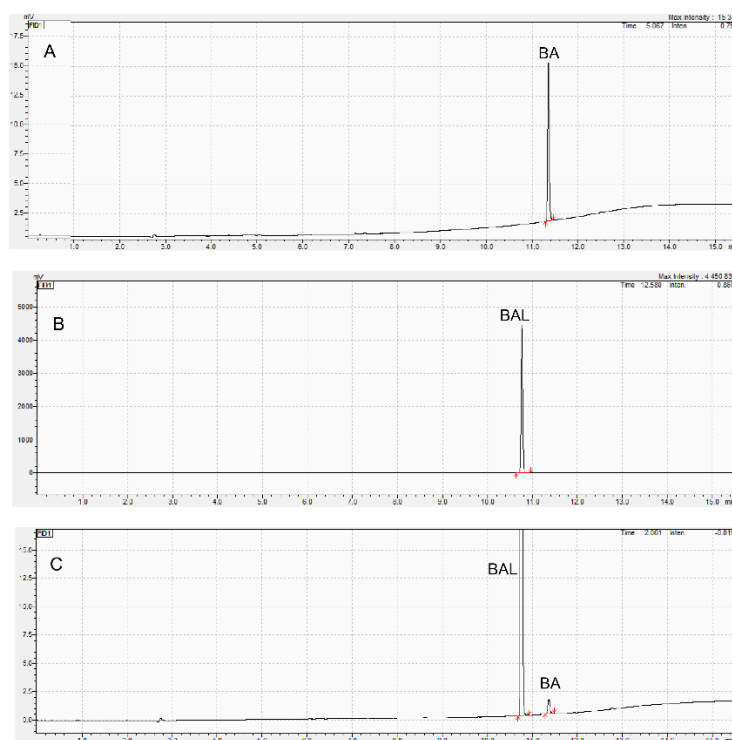


Fig. S6 An example of product determination during the photocatalytic evaluation of d-CN in the presence of BA in water at 455 nm. BAL is determined chromatographically. At 3 h of irradiation, nearly all BA reactants are oxidized to BAL (>97% BA conversion) with selectivity and aromatic balance close to unity (>99%), demonstrating that the aromatic ring remains intact while the -OH group is selectively oxidized to -CHO. (A) BA (1 mmol L^{-1}) in Milli-Q water, (B) BAL (1 mmol L^{-1}) in Milli-Q water, and (C) BAL detected in the reaction solution at 3 h, with <3% of BA remaining.

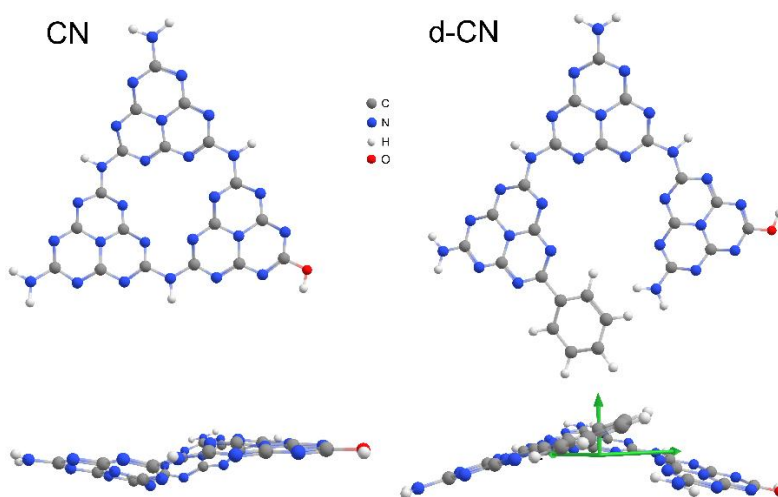


Fig. S7 DFT-optimized structures of CN and d-CN clusters.

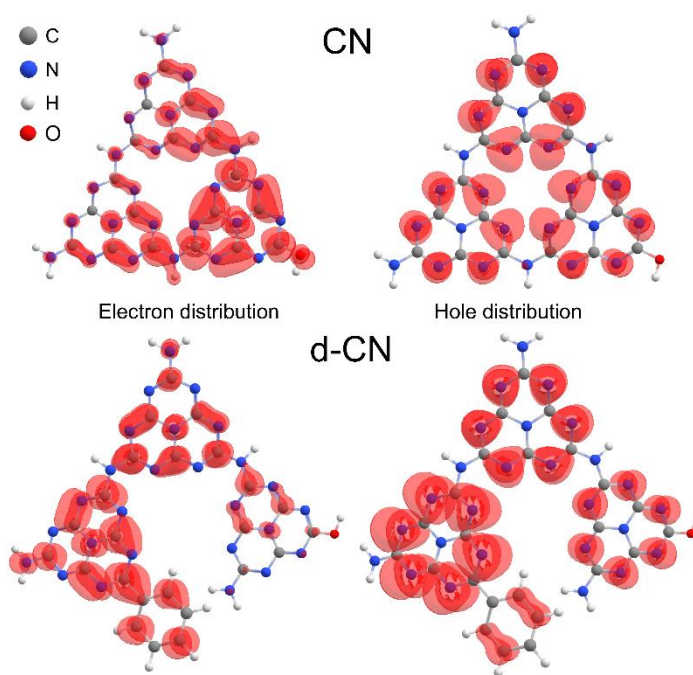


Fig. S8 First excited state of the electron-hole distribution of CN and d-CN clusters calculated with TD-DFT.

Table S1 Performance comparison of photocatalysts based on carbon nitrides for H₂O₂ production.

Photocatalyst	Yield / $\mu\text{mol h}^{-1}$	Light source	Electron donor	Photocatalyst dose / g L^{-1}	Ref.
Perylene imides-grafted C ₃ N ₄	60	300 W Xe lamp		1	14
CoP-loaded C ₃ N ₄	70	300 W Xe lamp	Ethanol	1	15
Biphenyl diimide-grafted C ₃ N ₄	10	Solar simulator		1.7	16
CN _{QDs} -loaded melamine-Ag	40	300 W Xe lamp	Isopropanol	1	17
P-doped C ₃ N ₄	90	350 W Xe lamp	Isopropanol	0.5	18
P-doped C ₃ N ₄	125	350 W Xe lamp		1	19
Au-loaded C ₃ N ₄	100	300 W Xe lamp	Ethanol	4	20
CoWO/C ₃ N ₄	10	300 W Xe lamp		1	21
Ti ₃ C ₂ /C ₃ N ₄	2	300 W Xe lamp	Isopropanol	1	22
BN _{QDs} -C ₃ N ₄	72	300 W Xe lamp	Isopropanol	1	23
B-doped C ₃ N ₄ @Bi ₂ S ₃	42	300 W Xe lamp		1	24
Polydopamine-grafted C ₃ N ₄	23	300 W Xe lamp		1	25
Bromo uracil-grafted C ₃ N ₄	126	50 W LED lamp	Isopropanol	1	26
Phenyl-grafted C ₃ N ₄	760	0.45 W LED lamp	Benzyl alcohol	0.5	This work

References

- D. A. Giannakoudakis, A. Qayyum, M. Barczak, R. F. Colmenares-Quintero, P. Borowski, K. Triantafyllidis and J. C. Colmenares, *Applied Catalysis B: Environmental*, 2023, **320**, 121939.
- A. Qayyum, D. A. Giannakoudakis, D. Łomot, R. F. Colmenares-Quintero, A. P. LaGrow, K. Nikiforow, D. Lisovytskiy and J. C. Colmenares, *Ultrasonics Sonochemistry*, 2023, **94**, 106306.
- A. U. Khan, R. A. Khera, N. Anjum, R. A. Shehzad, S. Iqbal, K. Ayub and J. Iqbal, *RSC Advances*, 2021, **11**, 7779-7789.
- M. Ibarra-Rodriguez and M. Sánchez, *Adsorption*, 2020, **26**, 597-605.
- F. Neese, *Journal of Computational Chemistry*, 2023, **44**, 381-396.
- F. Neese, F. Wennmohs, U. Becker and C. Riplinger, *The Journal of Chemical Physics*, 2020, **152**.
- T. Lu, *The Journal of Chemical Physics*, 2024, **161**, 082503
- T. Lu and F. Chen, *Journal of Computational Chemistry*, 2012, **33**, 580-592.
- G. Andrienko, www.chemcraftprog.com, 2010.
- J. Choi, B. H. Suryanto, D. Wang, H.-L. Du, R. Y. Hodgetts, F. M. Ferrero Vallana, D. R. MacFarlane and A. N. Simonov, *Nature communications*, 2020, **11**, 5546.
- G. Liao, C. Li, X. Li and B. Fang, *Cell Reports Physical Science*, 2021, **2**, 100355.
- S. Wu and X. Quan, *ACS ES&T Engineering*, 2022, **2**, 1068-1079.
- X. Xiao, J. Jiang and L. Zhang, *Applied Catalysis B: Environmental*, 2013, **142**, 487-493.
- L. Yang, G. Dong, D. L. Jacobs, Y. Wang, L. Zang and C. Wang, *Journal of Catalysis*, 2017, **352**, 274-281.
- Y. Peng, L. Wang, Y. Liu, H. Chen, J. Lei and J. Zhang, *European Journal of Inorganic Chemistry*, 2017, **2017**, 4797-4802.
- Y. Kofuji, S. Ohkita, Y. Shiraishi, H. Sakamoto, S. Tanaka, S. Ichikawa and T. Hirai, *ACS Catalysis*, 2016, **6**, 7021-7029.
- M. Yin, X. Chen, Y. Wan, W. Zhang, L. Feng, L. Zhang and H. Wang, *ChemCatChem*, 2020, **12**, 1512-1518.
- X. Dang, R. Yang, Z. Wang, S. Wu and H. Zhao, *Journal of Materials Chemistry A*, 2020, **8**, 22720-22727.
- J. Zhang, J. Lang, Y. Wei, Q. Zheng, L. Liu, Y.-H. Hu, B. Zhou, C. Yuan and M. Long, *Applied Catalysis B: Environmental*, 2021, **298**, 120522.
- G. Zuo, S. Liu, L. Wang, H. Song, P. Zong, W. Hou, B. Li, Z. Guo, X. Meng and Y. Du, *Catalysis Communications*, 2019, **123**, 69-72.
- S. Zhao and X. Zhao, *Applied Catalysis B: Environmental*, 2019, **250**, 408-418.
- Y. Yang, Z. Zeng, G. Zeng, D. Huang, R. Xiao, C. Zhang, C. Zhou, W. Xiong, W. Wang and M. Cheng, *Applied Catalysis B: Environmental*, 2019, **258**, 117956.
- Y. Yang, C. Zhang, D. Huang, G. Zeng, J. Huang, C. Lai, C. Zhou, W. Wang, H. Guo and W. Xue, *Applied Catalysis B: Environmental*, 2019, **245**, 87-99.
- S. M. Ghoreishian, K. S. Ranjith, M. Ghasemi, B. Park, S.-K. Hwang, N. Irannejad, M. Norouzi, S. Y. Park, R. Behjatmanesh-Ardakani and S. M. Pourmortazavi, *Chemical Engineering Journal*, 2023, **452**, 139435.
- Z. Gong, L. Chen, K. Chen, S. Gou, X. Zhao, L. Song, J. Ma and L. Han, *Journal of Environmental Chemical Engineering*, 2023, **11**, 109405.
- T. Bhojar, B. M. Abraham, A. Gupta, D. J. Kim, N. R. Manwar, K. S. Pasupuleti, D. Vidyasagar and S. S. Umare, *Journal of Materials Chemistry A*, 2024, **12**, 979-992.